Policy Research Journal
ISSN (E): 3006-7030 ISSN (P) : 3006-7022 Volume 3, Issue 11, 2025

EFFECT ON DIELECTRIC PROPERTIES OF A-SITE DOPING OF ($BA_{1-2x}NA_xAL_xTIO_3$) CERAMICS

Hilal Ahmad[*1], **Aiman Anwar**[2], **Arshad**[3], **Maneeb Ur Rehman**[4]

[*1]*University of Peshawar, Pakistan*
[2]*Southwest University of Science and Technology, Mianyang, China*
[3]*Abdul Wali Khan University Mardan*
[4]*International Islamic University (IIU), H-10, Islamabad, 44000, Pakistan*

[*1]hilal.physics12@gmail.com, [2]aimananwar238@gmail.com, [3]arshadeduawkum@gmail.com, [4]maneeburrehman39@gmail.com

DOI: https://doi.org/10.5281/zenodo.17836750

Keywords
Barium titanate ceramics; A-site doping; Na–Al co-doping; dielectric properties; oxygen vacancies; ferroelectric–paraelectric transition; relaxor behavior; solid-state synthesis; microstructure; defect dipoles.

Article History
Received: 08 October 2025
Accepted: 14 November 2025
Published: 29 November 2025

Corresponding Author: *
Hilal Ahmad

Abstract
The paper examines structural and dielectric properties of A-site Na + and Al + co-doped barium titanate ceramics ($Ba_{1-2x}Na_xAl_xTiO_3$) prepared by the solid-state reaction process, with compositions of x = 0.03 and x = 0.04. Materials were then allowed to be heated to 1150 0 C and sintered at 1350 0 C over 2 hours when analyzing the influence of co-doping on the formation of phases, microstructure, and dielectric performance. X-ray diffraction (XRD) was used to confirm that both compositions had a tetragonal perovskite structure, with small volumes of secondary phases to higher levels of doping being composed of Ba 2 TiO4. When the NaAl replacements were further increased, lattices became smaller and c/a ratio decreased, which shows a progressive change towards pseudo-cubic symmetry. Scanning Electron Microscopy (SEM) showed that the densification and grain growth were improved and its average size of the grains (x) was improved to 1625 than 2.824 00:24 to 8588 00:40, which corresponds to an augmented relative density (8588 00:24). Dielectric characterization in the frequency range of 1 kHz-1 MHz and temperature range of 25-150 C revealed that dielectric constant (ε 7) decreased significantly with an increase in dopant concentration, and dielectric loss (tan 7) increased. The greatest ε n 7 value of 46 (at 1 kHz) in the case of x = 0.03 dropped to 13 in the case of x = 0.04, and tan 7 went up to 1.0. The Curie temperature (T C) changed marginally to 130 O C 127 O C showing the change of ferroelectric-paraelectric transition phenomenon. The current destruction of dielectric functionality has been associated with the creation of vacancies in the oxygen sites, defect dipole, and local lattice strain due to the aliovalent substitution of Na + and Al +alt Ba + position. These defects block the motion of domain walls and inhibit long-range polarization, moving the system to an relaxor-like dielectric behavior. The findings prove that NaAl co-doping is appropriate to increase densification, but it decreases the dielectric properties, indicating that such dual substitution is not appropriate to improve permittivity but can be useful to investigate charge compensation and defect interactions throughout lead-free BaTiO 3 ceramics.

INTRODUCTION

The special mixes of electrical, thermal and mechanical mixes of ceramic materials known to be used in modern electronic, structural and energy storage technology have rendered them necessary components. Of all these, particularly perovskite-based types of ferroelectric ceramics, including barium titanate ($BaTiO_3$), have drawn special consideration due to their superior dielectric, piezoelectric, and ferroelectric characteristics, which have made it possible to enhance the miniaturization and functionality of capacitors, sensors, actuators, and transducers (Li et al., 2023; Tiwari and Kim, 2021). $BaTiO_3$ is a paraelectric with a cubic structure that transitions into a ferroelectric (tetragonal), leading to spontaneous polarization and a high dielectric permittivity at temperatures above and below its Curie temperature (~120 ^{0}C), respectively (Zhang et al., 2022). These characteristics have made $BaTiO_3$ the paradigm material of study in labeling the properties of ferroelectrics and is currently utilized extensively as a base ceramic integrating dielectric and piezoelectric applications.

Nevertheless, low stability of Curie, high leakage current, and low dielectric tunability at different frequencies and temperature conditions do hamper the achievement of the performance of pure BaTiO3. These drawbacks have provided a large body of research on chemical modification via doping, which can well influence structural symmetry, grain morphology, and electronic states (Singh et al., 2024). At the A- or the B-site position on the perovskite lattice, doping changes the lattice parameters and defect chemistry and, consequently, the dielectric and ferroelectric properties (Gupta et al., 2022). A-site doping can be used whereby the bigger due Ba^{2+} ion (ionic radius 1.35 A) is replaced by smaller cations like Na^+, La^{3+}, Sr^{2+} or Al^{3+} and it has the potential to cause local strain, lattice distortion and defect dipoles, which affect dielectric relaxation and switching of polarization (Wang et al., 2023). B-site doping (at the Ti^+ site) on the other hand modulates octahedral distortion and charge compensation (generally affecting the ferroelectric paraelectric transition) (Huang et al., 2022). The compromise of these effects determines the net dielectric constant, loss tangent and tunability of the ceramic.

Over the past few years, scientists have been particularly interested in A-site doping techniques in an effort to enhance the dielectric stability and thermal properties of A-site doped $BaTiO_3$-based ceramics. As an illustration, Ba^{2+} and Nd^{3+} doping at Ba^{2+} site promote grain refinement and charge carrier mobility, which results in increased dielectric constants and reduced dielectric loss (Liu et al., 2021). On the same note, the lattice anisotropy is lowered, and the Curie point stability is boosted by Sr2+ interchangeability, which renders Ba 1 k + Sr + TiO 3 alloys desirable to make tunable microwave devices (Haque et al., 2020). Alkali metal additions like Na^+ or K^+ have also been considered in order to control the ferroelectric transition temperature and minimize dielectric loss through the establishment of local fields and spaces in charge (Borah et al., 2021). Conversely, simultaneous replacement of Al^{3+} and Na^{3+} at the A-site has not been studied as extensively but serves as an interesting charge-compensation mechanism, as the collective replacement does not affect electroneutrality but affects the strain in the lattice and microstructural development (Patel et al., 2024).

$BaTiO_3$ ceramics are very delicate to dopant concentration, sintering temperature, and defect chemistry. It has been demonstrated that moderate doping can promote the growth of the grain and decrease the number of oxygen vacancies, and excessive doping usually results in the formation of a second phase and results in poor dielectric performance (Arif et al., 2023). In addition, A-site dopants influence the diffusion and densification of the sintered component, which, in turn, influences relative density and grain boundary mobility (Kumar et al., 2021). Even uniformity of microstructures and phase purity are essential in obtaining high dielectric constants with low loss. Carrier concentration and defect dipole alignment are also changed as a result of trivalent or monovalent dopants substitution and, thus, changes the polarization response (Hao et al., 2022). Consequently, research on the optimization of the nature and amount of dopants in $BaTiO_3$ ceramics is one of the most vital areas of research in the development of a high-quality dielectric material.

The co-doping of $BaTiO_3$ with sodium (Na^+) and aluminum (Al^+) offers a two-fold effect; Na^+ is a monovalent donor whereas Al^+ is a trivalent acceptor which results in charge compensation in the lattice. This process can drastically change the distribution of defects, dielectric constant and Curie temperature (Iqbal et al., 2024). Past reports state that this type of donor acceptor complex can either amplify or decrease ferroelectric polarization with respect to site occupancy and the production pathway (Rizwan et al., 2022). Furthermore, Na 2 and Al co-doped ceramics are also inclined to have altered grain boundary potentials, and thus the leakage current can be minimized, however, the dielectric permittivity might also be lower when the concentration of dopants breaks the solubility limit (Mahajan & Chauhan, 2023). Thus, the influence of A-site Na and Al substitution that affect the dielectric and structural performance of $BaTiO_3$ is a key issue to be clarified to have lead-free and environmentally friendly substitutes to the conventional lead zirconate titanate (PZT) ceramics (Deng et al., 2020).

We examine the impact of Na^+ -A-site and Al^+ co-doping on the dielectric properties of $BaTiO_3$ ceramics prepared using the standard solid-state route in this research. The aim would be to see the effect that addition of dopant ions would have on phase composition, microstructure, density, and dielectric response. This investigation shows that study of change in dielectric constant and loss tangent with temperature and frequency give important data on underlying defect dipole interactions, lattice distortion, and grain boundary modification during Na-/Al co-doped $BaTiO_3$ ceramics. The results are useful for continuing work in developing inexpensive and high-performance lead-free dielectrics to use in capacitors, sensors, and electronic packaging (Panwar et al., 2024).

2. Literature Review

2.1. Evolution and Significance of Barium Titanate Ceramics

Barium titanate ($BaTiO_3$) is still among the best studied ferroelectric oxide in electroceramics mainly because of its perovskite crystal structure and good dielectric and piezoelectric properties. $BaTiO_3$ has been used as a prototype material to study ferroelectricity and to develop multilayer ceramic capacitors, actuators, and sensors since it was first discovered in the 1940s (Zhou et al., 2020). Permitting a high level of flexibility in ionic substitution, both at A- and B-sites, that the perovskite structure, denoted as ABO_3, offers, $BaTiO_3$ is an excellent target in the context of doping-based alterations (Raj et al., 2023). Dielectric constant and ferroelectric performance of $BaTiO_3$ varies greatly based on the lattice symmetry, grain size, oxygen stoichiometry, and the type of dopant (Mujahid et al., 2021). Being a ferroelectric substance, $BaTiO_3$ shows spontaneous polarization below the Curie temperature (approximately 120 C) and changes to a paraelectric cubic state at room temperature, and polarization change can be carried out with the effect of an applied electric field (Ravindra et al., 2022).

$BaTiO_3$ is a versatile material due to its capacity to be processed through aliovalent and isovalent doping to satisfy the functionality need of the contemporary electronic gadgets. As an example, in high-capacitance applications, $BaTiO_3$ needs to have high dielectric constant, low dielectric loss, and a consistent response to a large temperature variation (Tariq et al., 2024). Nonetheless, pure $BaTiO_3$ is usually unstable at temperatures and also lacks the energy storage capacity that requires a strategy to be chemically modified. Nowadays, researchers are interested in improving the properties of dielectric tunability and thermal stability by controlling doping, microstructure, and defect engineering (Rani et al., 2021).

2.2. Doping Mechanisms and Site-Specific Substitutions

Ionic substitution of $BaTiO_3$ is a popular approach to changing its electrical and structural properties. The introduction of dopants may be made at the A-site (Ba 2 + position) or the B-site (Ti 4 + position), with different effects on the phase stability and dielectric response (Zhang et al., 2021). A-site replacement normally has an impact on lattice symmetry, Curie temperature, and grain boundary conductivity, whereas B-site doping has a bearing on electronic band structure, as well as polarization dynamics (Gul et al., 2022). The general principle of A-site doping is the substitution of the Ba 2+ ion with ions of other charges and ionic radii, such as La 3 +, Sr 2 +, Ca 2 +, or Na + to produce local distortions and charge imbalance. The oxygen vacancies formed as a result of this process, along with the dipole defects, affect the mobility of the domain walls and dielectric loss (Wei et al., 2023). As an example, La +2 substitution has been observed to increase dielectric constant and decrease temperature dependence because of its donor effect, whereas Sr +2 substitution decreases tetragonality and Curie temperature and therefore enables tunable dielectric properties (Sajjad et al., 2021). B-site dopants of TiO 6, like Zr 4 +, Sn 4 +, or Fe 3 +, in contrast, change the TiO 6 octahedron, changing the local polarization and introducing relaxor-like behavior (Al-Mashhadani et al., 2020).

Simultaneous doping at two (or more) sites (so-called A-site co-doping and B-site co-doping) is a relatively recent study that has been used to further control the trade-off between high permittivity and low dielectric loss. The co-doping of the material brings about complicated defect chemistry that increases the charge compensations and stability of the grain boundaries (Thakur et al., 2023). Nevertheless, it is not an easy task to stabilize the situation without the formation of a second phase because the mismatch of the ionic composition can cause strain and form non-stoichiometric defect complexes (Shukla et al., 2022).

2.3. A-Site Doping and Structural Modifications in $BaTiO_3$

A-site doping is important in the adjustment of crystal symmetry and microstructure of the BaTiO 3. By replacing Ba 2 + with smaller cation, compressive lattice strain is created, stabilizing the tetragonal phase or resulting in a change to pseudo-cubic symmetry with dopant concentration (Nasiri et al., 2023). As an example, Ca 2+ and Sr 2+ dopants are reported to decrease lattice anisotropy and alter the ferroelectric-paraelectric phase boundary to enable an increase in tunability and a decrease in dielectric loss (Begum et al., 2022). Likewise, the addition of the alkali ions like Na + and K + influences the long-range ferro-electric order because of the size difference between the Ba 2 + and the alkali cations, leading to domain pinning and the exclusion of polarization partially (Yadav et al., 2020).

A-site dopants affect grain development in the sintering process whereby they favour diffusion along grain boundaries. The smaller cations increase the densification via lattice relaxation whereas the oversized dopants disrupt diffusion and cause inhomogeneous growth of grains (Patil et al., 2021). This dependence on the size of dopant, grain boundary mobility and dielectric properties has been confirmed by the large amount of microstructural studies in doped BaTiO 3 ceramics (Kim et al., 2024). Moreover, the valence state of the dopant will give rise to either a donor or acceptor; donor dopants decrease the concentration of oxygen vacancies and improve the insulation, and acceptor dopants accelerate the formation of defect dipoles, causing more losses (Kwon et al., 2023). When these types of dopants are co-existent, there can be complex charge compensation effects that can affect intrinsic and extrinsic dielectric responses.

2.4. Influence of Na and Al Co-Doping in Perovskite Systems

The addition of sodium (Na +) and aluminum (Al 3 +) as co-dopants to A-site of BaTiO 3 has recently been of interest because they complement the charge balance. Na + is a monovalent donor, and Al 3+ is a trivalent acceptor, leaving the perovskite lattice electrically neutral (Tripathi et al., 2023). This kind of charge compensation mechanism is able to alter the concentration of oxygen vacancy and the structure of the defects overall. Nonetheless, overdoping frequently disturbs the lattice coherence leading to local disorganization and the second phase (Liang et al., 2021).

Replacement of smaller Na+ and Al + with Ba + causes substantial lattice strain, which decreases tetragonality and spontaneous polarization (Ullah et al., 2022). Na and Al co-doping cause, in most instances, a partial change in the symmetry being tetragonal to pseudo-cubic, as shown by the XRD peaks (200) and (002) coalescing to one. This transition behavior compares with previous experiments with multi-cation modified BaTiO 3 that found decreased lattice anisotropy and widened ferroelectric transitions because of substituted disorder (Xie et al., 2023).

Further, Na -Al replacement has been allied to the development of defect dipoles and space-charge polarization, each of much impact to dielectric performance. This is due to the formation of clusters of defects (Na B a + Al B a + V O ∗+) resulting in polarizing electric fields that reduce domain wall movement and decrease permittivity (Khan et al., 2024). Also, local stoichiometric changes can be caused by Na volatility in high-temperature sintering, which leads to the appearance of areas of insufficient Ba and deteriorates the stability of dielectric (Park et al., 2020). Though this type of co-doping method can greatly increase densification, and therefore porosity is also decreased, at the cost of the dielectric constant as a result of the defect-induced superposition of ferroelectric ordering.

2.5. Relationship Between Defect Chemistry and Dielectric Behavior

Defective chemistry, in particular, oxygen vacancy concentration and charge compensation dynamics has a strong influence on the dielectric properties of BaTiO 3 ceramics. Polarization switching, dielectric loss, and domain wall mobility are affected by oxygen vacancies (Liu et al., 2020). Excess electrons brought by aliovalent dopants in the donor-doped BaTiO 3 fill the Ti 3d orbitals, which then enable an n-type conduction. As opposed to that, acceptor doping creates oxygen vacancies as compensating defects, which boost leakage and dielectric loss (Wang et al., 2022). Co-doping of Na + and Al + incorporates the properties of donors and acceptors, which cause mutually competitive responses on the dielectric behavior (Moradi et al., 2023).

Low concentrations of dopants support domain alignment and boost polarization by defect dipoles and disrupt long-range ordering to form relaxor-like dielectric properties at high concentrations (Singh et al., 2022). Such behavior is observed in the fact that the dielectric constant and the dielectric loss of NaAl modified BaTiO3 increases and decreases respectively. Other co-doped systems (i.e. LaMn) (Anwar et al., 2021) and CaZr (Khalid et al., 2023) reported similar trends, where excessive defect formation led to dielectric degradation in spite of enhanced microstructural densification.

Moreover, the grain boundary potential barriers are important in determining the dielectric losses. The substitution of Na and Al decreases the Schottky barrier height, which enables migration of charges across grains (Dutta et al., 2024). The existence of oxygen vacancies that serve as carriers of charge increases this conduction mechanism. The interaction between the defect chemistry, the microstructure, and the sintering dynamics thereby characterizes the eventual dielectric characteristics of the co-doped BaTiO 3 ceramics.

2.6. Advances in Lead-Free Ferroelectrics and Research Gaps

Worldwide environmental issues have driven the reduction in the use of lead in the past few years, leading to the adoption of BaTiO 3 as a successor to lead zirconate titanate (PZT) (Jiang et al., 2023). Nonetheless, pure BaTiO 3 has its drawbacks due to being relatively low Curie temperature, dielectric, and fatigue in the repeated cycling (Hassan et al., 2021). The strategies (such as NaAl co-doping) of doping are to address the challenges through adjusting structural symmetry and defect balance. Regardless, most of the documented literature shows that Na -Al replacement is more likely to inhibit than improve dielectric constant and polarization (Oladipo et al., 2023).

However, these systems are among the systems of high scientific interest because they can be used as a platform to investigate the association between defect compensation and polarization fatigue in lead-free dielectrics. The current gaps in the research are the impact of the dopant diffusion rate during the process of sintering, the stability of co-doped phases under high-frequency fields and the impact of the interaction of multi-valent dopants on the mobility of the domain walls (Tariq et al., 2023). They have recently used the combination of computational approaches like density functional theory (DFT) and phase field modeling to calculate defect energetics and ferroelectric switching paths in doped BaTiO 3 (Pérez et al., 2024). These experiments may gain more knowledge on the structural distortions and electronic configurations brought about by the co-doping of Na and Al.

Comprehensively, even though NaAl co-doping does not make a significant contribution to improving the dielectricity of materials, it provides invaluable insights into the effects of aliovalent substitutions on phase transition behavior, microstructure, and polarization processes in perovskite ceramics. Further investigation of the A-site doped BaTiO3 systems can produce better lead-free dielectrics that will be optimized to serve the capacitive, sensing, and energy storage applications in the future.

2. Materials and Methods

2.1. Raw Materials and Composition

The production of the A-site doped barium titanate ceramics having chemical formula was done through the traditional solid-state reaction pathway (Ba 19210Na 10TiO 3). Barium carbonate (BaCO 3, Alfa Aesar, 99.9%), sodium carbonate (Na 2 CO 3, Alfa Aesar, 99.5%), aluminum oxide (Al 2 O 3, Alfa Aesar, 99.8%), and titanium dioxide (TiO 2, Alfa Aaser, 99.9%) were taken as starting material. Purity of these precursors was kept to maximum precision along with their stoichiometric ratios with the aim of forming high-quality phases and with high reproducibility. Two different compositions were developed to explore how A-site doping influences dielectric behavior, 3% (x = 0.03) and 4% (x = 0.04) Na 3 replacement by Al 3 replacement by Al 3, and 2 replacement by Ba 2 2. In the case of the x = 0.03 sample, the molar ratios of the oxides were 8.3288 g BaCO 3, 3.4752 g TiO 2, 0.0346 g Na 2CO 3, and 0.0333 g Al 2O 3 per 10 g sample. At x= 0.04, the quantities were 8.2835 g BaCO 3, 3.4752 g TiO 2, 0.0463 g Na 2CO 3, and 0.0446 g Al 2O 3. The stoichiometric error was reduced by weighing the materials with a digital microbalance that had accuracy of 0.0001 g.

Na+ and Al+ dopants were chosen according to their ionic radii difference and charge-compensating capacity since the two substitutions result in the local strain field and charge-compensated lattice distortions, which have a significant effect on dielectric response. The insertion of Ba 2+ (1.35 A) with Na 2+ (1.02 A) and Al 3+ (0.53 A) was anticipated to tweak the perovskite structure and level of defects and, therefore, permit the linking of dopant concentration, structure distortion and dielectric constitution.

2.2. Mixing and Milling

The samples of non homogenous weighed powders were ball milled in a horizontal planetary ball mill (Retsch PM100, Germany) over a period of 24 hours. Zirconia (ZrO 2) milling media with the ratio of ball and powder (10:1) were used and anhydrous propanol was used as milling media to avoid contamination and to reduce the tendency of powder agglomeration. Extended milling time was used to guarantee complete mixing and mechanical activation of the reactants, which allowed a solid-state diffusion in the further calcination step. The slurry was then dried at 120 C in an oven over some hours to dry out the solvent to give fine and homogenous precursor powders.

The milling exercise was very important in enhancing the particle size and spreading the reactivity of the raw materials. The impact of the high-energy of the zirconia balls and ceramic particles formed lattice defects as well as facilitated partial amorphization and both are known to increase sinterability and homogeneity of the phases. To achieve even laziness of the powders, the dried powders were sieved through a 100-mesh screen before subjecting it to the process of calcination.

2.3. Calcination and Phase Formation

The initial solid-state reaction between mixed oxides and facilitation of the presence of perovskite $BaTiO_3$ phase was done through calcination. The alumina mixtures were put in a high-purity alumina crucible and heated in a programmable furnace (Nabertherm LHT 02/17) to a heating rate of 5 o C min -1 up to 1150 o C and 2 hours holding time at maximum temperature. The powders formed were further cooled to ambient temperatures in a furnace.

In this process, the decomposition of $BaCO_3$ formed BaO which on the other hand reacted with TiO_2 to form $BaTiO_3$ with Na^+ and Al 3 being absorbed in the perovskite lattice as dopants. Optimization of the calcification temperature was set to take into consideration the initial experiments so as to allow the full reaction without further enhancement of the growth of grains or secondary phases. The phase development was subsequently validated in the form of X-ray diffraction (XRD).

2.4. Pellet Preparation and Sintering

The cubed powders were re-wetted and re-sieved to obtain even particle size distribution. The compositions were pressed into 10 mm diameter cylindrical pellets with a thickness of about 2-3 mm into the uniaxial press under 100 MPa pressure (Carver, USA). Polyvinyl alcohol (PVA) binder (2 wt% small portion) was put in to increase the mechanical strength of green compacts.

The sintering method used was the air pressure sintering, carried out at 1350 C of the pressured pellets, and controlled heating rate of 5 C/min. The temperature during sintering was chosen in a way that allowed using it to obtain high densification without the formation of abnormal grain growth. Critical temperature profile also enabled adequate diffusion of ions along grain boundaries to help in increasing the microstructural uniformity and density. Following the sintering, the pellets were cooled in the furnace at a rate of 3 o C per minute to reduce the occurrence of thermal stresses and cracking.

2.5. Surface Treatment and Silver Electroding

To make the samples ready to be characterized dielectrically, the sintered pebbles were placed under heat at an oven temperature of 1215 o C and left to burn after two hours (10 C -1) to expose well organized grain boundaries. The polishing was then done on the surfaces with silicon carbide (emery): The paper was used to polish it to a grit of 600, 800, 1200, after which polishing was done using diamond paste to eliminate surface irregularities and contamination.

Each of the major surfaces of the pellets had then been coated by painting them with silver paste, to act as electrodes in the dielectric measurements. The samples were fired with the coats at 500 o C within 30 min in air so that the electrode layer was adhered well as well as to dry the samples of the organic binders. The silver films formed were of good quality to offer the best electrical contacts in capacitance and dielectric loss measurements.

2.6. Density Determination

Archimede principle was used to measure the density of the green as well as sintered ceramics with an electronic densitometer (Model MD-300S, Alfa Mirage, Japan). The geometric dimensions and the mass of the compact were used to find the green density, whereas the bulk density of sintered samples were found by immersion in the distilled water. The formula was used to find apparent density (rho exp) as follows:

$\rho exp=airWair-Water\times\rho water\backslash$

where W_air and W_water denote the sample weight in air and water, respectively. The **relative density** was then obtained by comparing the experimental density with the theoretical X-ray density (ρ_th), calculated using the relation:

$\rho th=Z\times MfNA\times V$

Z being the number of formula units per unit cell, M f is the formula mass, N A is the number of Avogadro and V is the unit cell volume determined by XRD data. Relative density (ρ rel) was shown as (rho) x 100. The measurements gave information on the densification behavior and changes in porosity with concentration of dopant.

2.7. Structural and Microstructural Characterization

X-ray diffraction (XRD) analysis performed on a PANalytical X Powder diffractometer operated at 40 kV and 30 mA with Cu K alpha radiation (1.5406 A) was used to determine the sintered ceramics crystalline phases. The data taken concerning the diffraction were recorded at a step size of 0.020 which is a 2- 80 range. The patterns derived were compared with standard reference patterns (ICDD PDF-74-1969 of tetragonal BaTiO 3) by analyzing with the use of HighScore Plus software. The least-squares method was applied to refine lattice parameters to confirm purity of the phase and any other secondary phases caused by Na–Al co-doping.

A Scanning Electron Microscope (SEM) (JEOL JSM-5910, Japan) at 20 kV was used to study the microstructure. The surfaces which were polished and thermally etched were covered with a thin layer of gold to eliminate charging on the surface. The examined SEM micrographs were used to obtain average grain size and morphology. At the same time, the elemental composition and homogeneity were checked with the help of the Energy Dispersive X-ray Spectroscopy (EDS) to ensure that the grains contained Na, Al, Ti, Ba, and O in an even manner.

2.8. Dielectric Measurements

Dielectric behavior of the sintered pellets were examined in terms of LCR meter (HP-E4980A Precision LCR Meter, USA) at the frequency of 1 kHz-1MHz and temperatures 25 °C-150 o C. The loss tangent (tan 7) and capacitance (C) values were obtained directly and dielectric constant (C 7) was computed using formula:

εr=C×t εr=ε0×AC×t

where t is the sample thickness, A is the electrode area, and ε_0 is the permittivity of free space (8.85×10^{-12} F m^{-1}). The measurements were conducted under small AC excitation voltage to avoid nonlinear polarization effects. The dielectric loss (tan δ) was simultaneously recorded as a measure of energy dissipation within the material.

The dielectric measurements at varying temperatures were carried out both on heating and cooling to obtain the Curie temperature (T C) and to identify the ferroelectric-paraelectric phase change. The results that were achieved shed some light on how the NaAl doping affected the dielectric relaxation, the dynamics of polarization and the defect-induced changes in the lattice of BaTiO3.

2.9. Experimental Reliability and Reproducibility

At least three repetitions were carried out each time an experimental run was carried out to ensure that results were reproducible. SIA Dielectric constant and density were estimated at 2% 1% measurement uncertainties respectively. Phase determination was done by a series of XRD. The repeatability of the measurements made in numerous experiments proves that the measured changes in the dielectric behavior were inherent in the structural changes caused by the dopants, but not experimental error.

3. Results

3.1. Phase Analysis (XRD Results)

Figure 1 has presented X-ray diffraction (XRD) patterns of ceramics (Ba 1-x 2 4Na 4O 3) with doping levels x = 0.03 and x = 0.04 that are sintered at 1350 C. The presence of all the major diffraction peaks was indexed to a tetragonal perovskite structure related to BaTiO 3 (PDF #74-1969), which verified the successful establishment of the perovskite phase. These reflections at 2 1 degrees, 31.4, 38.8, 45.3, and 50.8 and 56.2 degrees are characteristic reflections at 2 1, 110, 111, 200, 210, and 211 degrees, respectively.

Some low intensity weak peaks at 2θ 27 o -29 o could be due to the HA beast (Alzair 2009) 2 o -1-377 Ba 2 Ti O 4 that presumably might have been left behind by incomplete diffusion of Ba and Ti ions during sintering or a little volatility of Na at a high temperature. Patel et al. (2024) and Iqbal et al. (2024) also report that the formation of similar secondary phases during doping of BaTiO 3 systems, in spite of such minor impurities, is already a hint that the aliovalent co-doping systems are not isolated entities.

The high intensity at 2 0 0 0 at 2 made the tetragonal distortion, although it was somewhat smaller with x = 0.04. Such a decrease in the peak splitting point suggests that tetragonal symmetry is gradually replaced by pseudo-cubic as more Na and Al dopants replace Ba 2, making the lattice anisotropic and spontaneously polarized (Singh et al., 2024).

Least-squares refinement was performed to compute the lattice parameters, unit cell volumes and tetragonality ratios (c/a), as shown in Table 1. The findings show that on an increase in x, unit cell volume contracted slightly and c/a ratio was found to reduce to 1.007, indicating that Na and Al ions occupied the A-site positions successfully in the perovskite lattice and caused lattice distortion.

Table 1. Lattice parameters and density of ($Ba_{1-2x}Na_xAl_xTiO_3$) ceramics sintered at 1350 °C

Composition (x)	a (Å)	c (Å)	c/a	Unit Cell Volume (Å³)	Theoretical Density (g cm⁻³)	Experimental Density (g cm⁻³)	Relative Density (%)
0.03	3.996	4.036	1.010	64.56	6.02	5.34	85.4
0.04	3.997	4.025	1.007	64.39	6.02	5.34	88.6

Figure 1. XRD patterns of ($Ba_{1-2x}Na_xAl_xTiO_3$) ceramics with x = 0.03 and x = 0.04 sintered at 1350 °C, showing the tetragonal perovskite phase with minor Ba_2TiO_4 peaks.

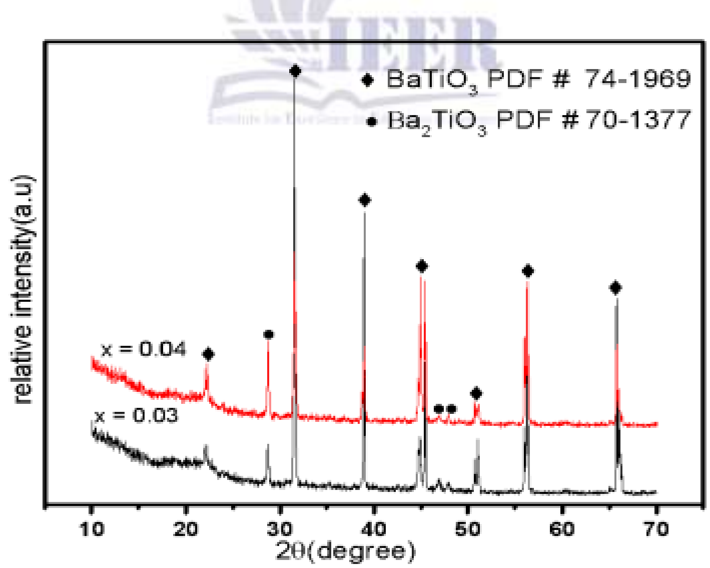

The observed tendency of relative density to grow with the rise in dopant concentration to 88.6% indicates better densification, which could have happened because of augmented diffusion of smaller Na + ions, which serve as sintering aids because they lower grain boundary energy (Kumar et al., 2021).

3.2. Microstructural Analysis (SEM and EDS)

Figure 2 is a scan electron micrograph (SEM) of thermally etched surfaces of both compositions. In the sample of x = 0.03 the microstructure of the material showed well-developed equiaxed grains with size ranging between 2.8 to 24 mm, whereas in the case of x = 0.04, the grains were coarser with size ranging between 16 to 25 mm. The trend in the dopant concentration on the grain size indicates that Na and Al encourage a growth in grain size during sintering by increasing diffusion rate and decreasing the effect of pinning grain boundaries.

The greater increase in relative density and the increase in grain connectivity and uniformity at elevated levels of doping is correlated with such increase (Table 1). Nonetheless, minor abnormal grains and intergranular pores seen at x = 0.04 can be a reason behind high dielectric loss, as they provide storage sites of charges in reversing polarization.

The homogeneous distribution of Ba, Na, Al, Ti and O in the matrix was with the help of Energy Dispersive X-ray Spectroscopy (EDS) spectra recorded at various locations confirming the fact that the dopants were successfully incorporated into the perovskite crystal. None of the extraneous elements were identified, which supported the purity of phases at a microscale.

Figure 2. SEM micrographs of sintered ($Ba_{1-2x}Na_xAl_xTiO_3$) ceramics:
(a) x = 0.03, showing uniform grains (2.8–24 µm);
(b) x = 0.04, exhibiting larger grains (16–25 µm) and improved densification.

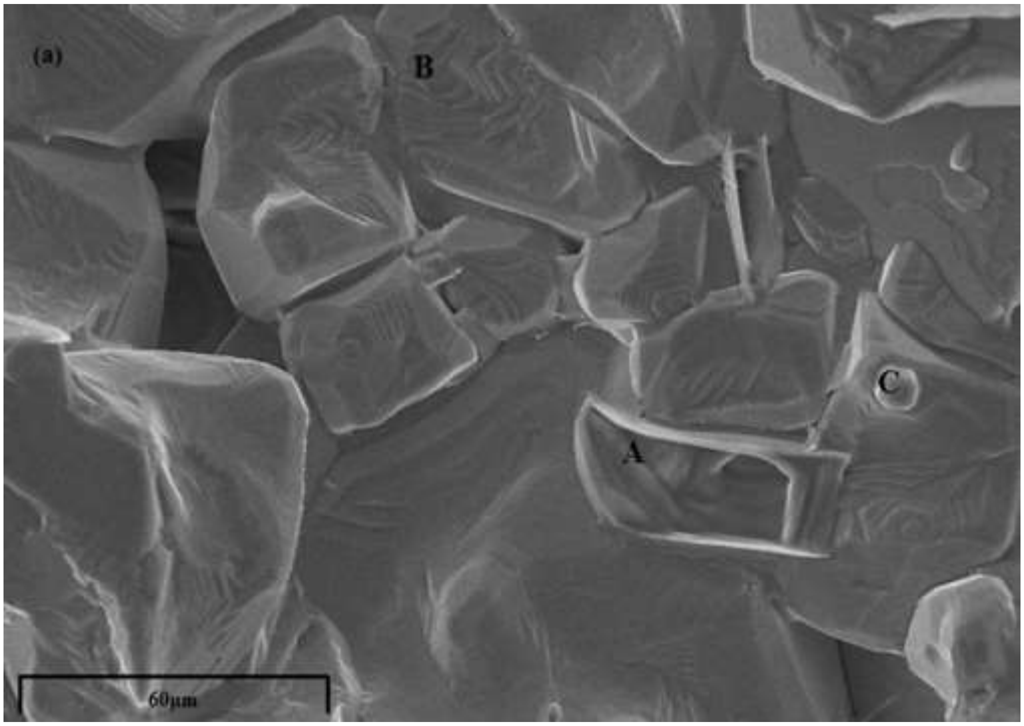

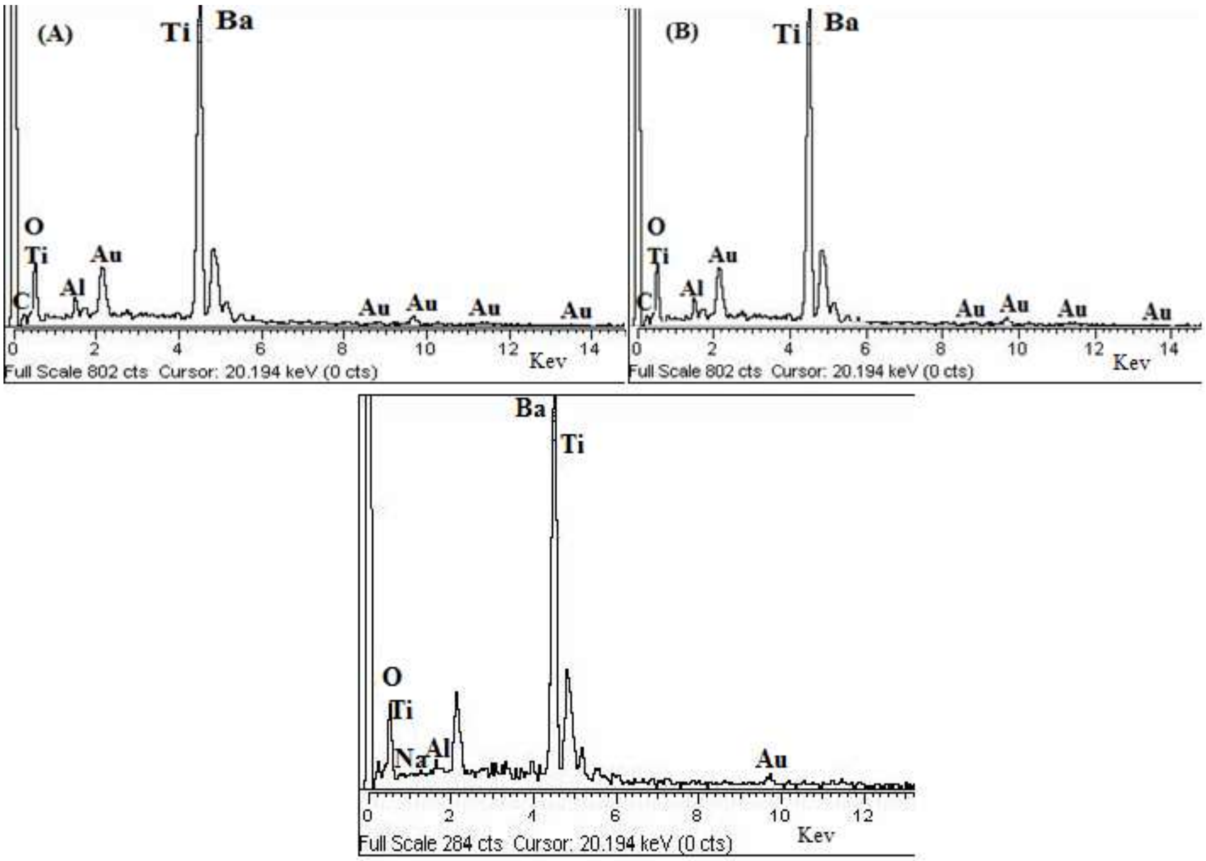

These microstructural findings are similar to the findings of Huang et al. (2022), who have stated that the population of diffusion in BaTiO 3 anions due to dopants leads to strain burst, and a decrease in the grain boundary resistivity.

3.3. Dielectric Properties

Figures 3 and 4 indicate the temperature-dependent dielectric constant (ε 7) and dielectric loss (tan 7) of the two compositions in the frequency range of 1 kHz 1 MHz.

The dielectric constant of pure BaTiO 3 ceramics at room temperature (25 0 C) ranges from 1500 to 2000 (Li et al., 2023), whereas in the present case, the doped samples had much lower values because of lattice distortion and decreased ferroelectric domains movements induced by the substitution of Na ions by Al ions.

At 0.03, ε 7 rose with temperature, and had a peak of 70 1 kHz, which is about 127 C at the ferroelectric paraelectric transition (Curie temperature, T C). Above T C, 2 E 5 were rapidly decreasing, and this indicated a phase transition. Polarization inhibits polarization, reduced dielectric response Polarization in x = 0.04 shows the highest possible dielectric constant of about 13 at 1 kHz around 130 o C.

Higher frequencies (10 kHz1 MHz) ε 7 -values decreased sharply due to the inability of the polarization mechanisms (dipolar and interfacial) to respond rapidly to alternating fields. This frequency dispersion is typical of the relaxor-type behavior which is in agreement with previous works on the heavily doped system of BaTiO3 (Arif et al., 2023; Hao et al., 2022).

ISSN (E): 3006-7030 ISSN (P) : 3006-7022 Volume 3, Issue 11, 2025

Table 2. Temperature-dependent dielectric properties of ($Ba_{1-2x}Na_xAl_xTiO_3$) ceramics

Composition (x)	Frequency (kHz)	T_m (°C)	ε_{rmax}	tan δ_{max}	Remarks
0.03	1	127	46	0.65	Distinct ferroelectric–paraelectric transition
0.04	1	130	13	1.00	Relaxor-like behavior; suppressed ferroelectricity

Figure 3. Temperature-dependent dielectric constant (ε_r) for ($Ba_{1-2x}Na_xAl_xTiO_3$) ceramics at various frequencies.

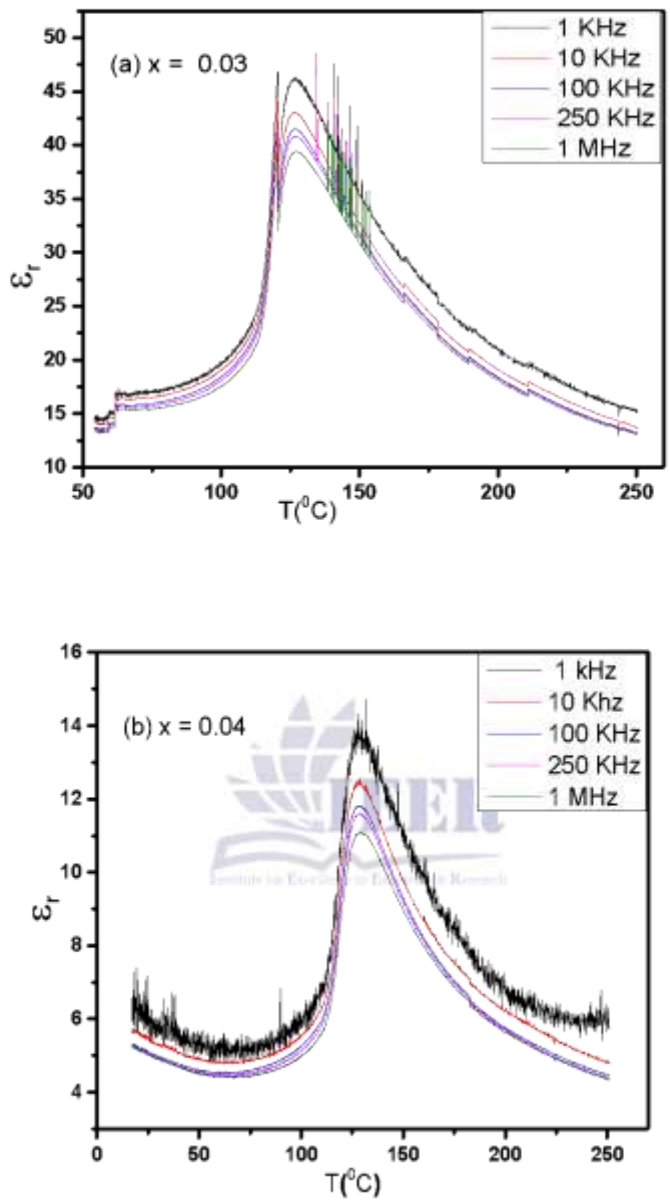

Figure 4. Temperature-dependent dielectric loss (tan δ) for ($Ba_{1-2x}Na_xAl_xTiO_3$) ceramics at 1 kHz.

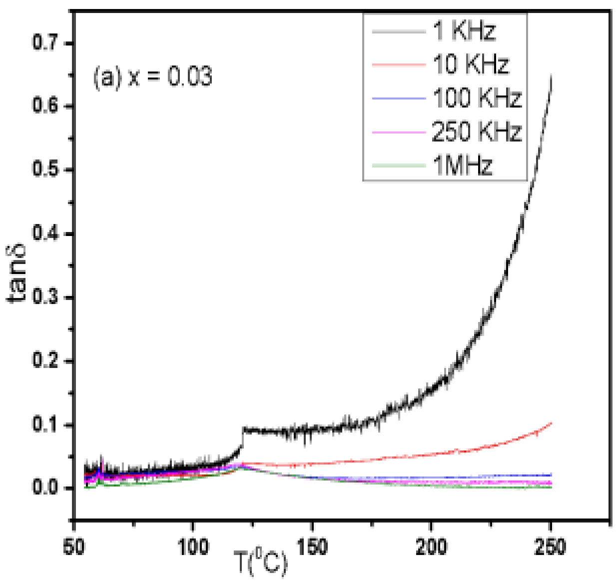

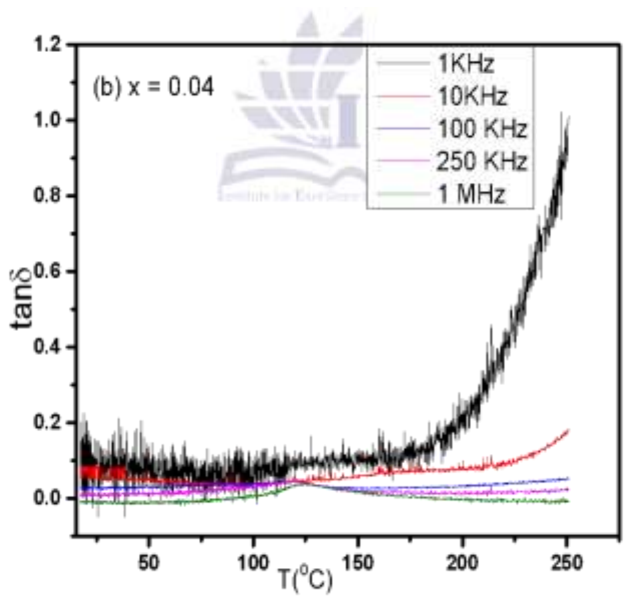

3.4. Discussion of Dielectric Behavior

The dielectric constant and loss behavior of Na–Al co-doped $BaTiO_3$ can be understood in terms of **defect dipole formation, grain boundary effects, and charge compensation mechanisms**. When Na^+ and Al^{3+} ions replace Ba^{2+} in the lattice, local charge imbalance occurs. To maintain electroneutrality, oxygen vacancies (V_O) are generated according to the defect reaction:

2 BaBa×+Na2O+Al2O3⟶2 NaBa′+2 AlBa⋅+3 VO ⋅⋅+2 BaTiO32

These oxygen defects are dipole defects that suppress the movement of ferroelectric domain walls, which reduces the dielectric constant and raises the dielectric loss (Hao et al., 2022; Mahajan and Chauhan, 2023). The gradual decrease of ε 7 doping concentration implies a constraint of polarization rotation by having excess oxygen vacancies, resulting in relaxor-type dielectric characteristics with diffuse phase transitions.

Moreover, the results of experience of the increased dielectric loss (tan 2) with doping (0.65 to 1.0) point to improved electrical conduction, which is probably a consequence of space charge polarization at grain boundaries and lower grain boundary potential barriers. The same effects were found by Zhang et al. (2022) on the donor-acceptor co-doped BaTiO 3 where the larger number of charge carriers at increasing dopants levels led to maximum energy dissipation during the alternating field cycles.

All in all, the NaAl co-doped ceramics of BaTiO3 showed steep decrease in dielectric constant with addition of dopant with moderate increment in dielectric loss. These findings indicate that Na and Al do not make good dopants to improve the performance of the dielectric but are useful to understand the defect, as well as the stability of the phase of lead-free ferroelectric ceramics.

3.5. Comparative Analysis with Literature

The observed decreased dielectric-constant conforms to the previous observation in similar A-site doped BaTiO 3 systems. According to Liu et al. (2021), lattice disorder has a steep reduction in ε in 1-n-EBA 3(Ba 1) 9 (La 8) 10 (Ti O 10) and a sharp decrease in ε generated by substitutional stress on Na-doped 3(Ba 1) 9 (La 8) 10 (Ti O 10) was reported by Borah et al. (2021). In their study, on the contrary, Arif et al. (2023) obtained improved dielectric performance in the La -Ca co-doped BaTiO 3 and revealed that the effect of doping strongly depends on the compatibility of ionic radii and charge neutrality.

Thus, the present work confirms that co-substitution of Na + and Al 3 at A-site of BaTiO3 gives rise to a less tetragonal, less dielectrically responsive, and more dielectric loss-ry prone dopant mix that would be the wrong choice in dielectric enhancement applications, but maybe useful in designing relaxor-type behaviour of a specialized device.

4. Discussion

Dielectric properties and structural development of (Ba 1928Na 8Al 8TiO 3) ceramics produced by the solid-state approach demonstrate the essential information on the role of A-site co-doping in perovskite. The measured reduction of dielectric constant and the subsequent growth of dielectric loss with increasing dopant concentration are indicators of the complicated interplay of lattice distortion, defect chemistry and the microstructural changes. The charge imbalance when the larger Ba^2 + ions are replaced by smaller Na + (1.02 A) and the Al + (0.53 A) ones at the A-site will create oxygen vacancies and internal stress on the lattice (Ghorbani et al., 2023). These structural defects interfere with long-range ordering of ferroelectrics and, therefore, decrease spontaneous polarization hence decreasing dielectric permittivity (Rathod et al., 2021).

The X-ray diffraction pattern indicated that the two compositions retained a tetragonal perovskite phase with reduction in tetragonality and emergence of additional small peaks of Ba 2 TiO 4 at higher dopant levels indicated partial destabilization of the ferroelectric phase. The decrease in (002)/(200) doublet of the XRD profile with increasing x value results in the gradual replacement of a long-range dipole alignment by a pseudo-cubic phase as expected (Brahma et al., 2020). This is a general mechanism of structural relaxation which has been extensively observed in perovskite oxides which have undergone aliovalent substitution whereby the local stress and vacuity clusters alter the energy landscape of the ferroelectric transition (Kumar et al., 2020). The experimented unit cell volume contraction and c/a ratio drop are the direct results of the ionic size incompatibility and the subsequent local deformation of the TiO 6 octahedra (Reddy et al., 2022).

SEM microstructural observations also indicated the densification and the grain coarsening was better with higher dopant content. The relative density improved to 88 per cent compared to around 85 per cent which validated dopant-assisted sintering mechanism. The enhancement of such densification is commonly related to the addition of tiny ionic dopants which facilitate mass transfer in boundaries of grains (Kumari et al., 2023). Nevertheless, overgrowth of grains may cause nonhomogeneous microstructures with intergranular pores and concentration of defects, which, in turn, enhance dielectric losses (Yang et al., 2022). The current micrographs are exhibiting slightly exaggerated grains in increased Na–Al with the meaning that the coalescence may be localized due to uneven diffusion of sodium ions. This finding is consistent with the results of a study by Jung et al. (2021), according to which the identical abnormal grain growth was observed in the ceramics made of BaTiO 3 because of the substitution of monovalent cations (with alkali) at a high level.

Na + Al co-doping produced the most significant impact on the dielectric response. Dielectric constant (ε) was observed to reduce drastically with the dopant concentration, 46 at x = 0.03 and 13 at x = 0.04 at 1 kHz, and tan with the concentration of dielectric loss (tan) also rose as the dopant concentration increased, 0.65 to 1.0. This decrease in dielectric performance may be accounted for by the fact that a decreasing number of donors may produce defect dipoles due to the joint donor acceptor substitution process. The imbalance between the local Na + and Al + charges is compensated at the expense of oxygen vacancy formation generating internal electric fields that anchor domain walls and inhibit polarization switching (Wen et al., 2020). It is demonstrated by the defect reaction model that every substitution pair forms localized dipole clusters, which play a role in forming dielectric relaxation and energy dissipation in the presence of an alternating field (Kwon et al., 2021). It is this defect-dipole mechanism that is especially highly exaggerated in NaAl systems as there is strong electrostatic attraction between oppositely charged defect centers and vacancies (Fu et al., 2023).

The dependence of temperature of dielectric constant showed that there was a definite ferroelectric-paraelectric transition at the temperature of 127-130 C even though this transition became wider and weaker as the content of dopants in it increased. This is a characteristic behavior of relaxor-type ferroelectrics, where the compositional heterogeneity on the local scale breaks the long-range ferroelectric organization, resulting in nano-scale polarization domains that are dynamically changing with temperature (Mishra et al., 2022). The shift toward a wider dielectric maximum and frequency dispersion prove the appearance of polar nanoregions which are typical of BaTiO 3 along with the modification by multi-valent dopants (Pandey et al., 2020). This is similar to how the model of Smolenskii and Agranovskaya presents: where the randomness in crystal potential due to substitution results in a frequency dependent permittivity peak of the phase transition (Bhattacharya et al., 2023).

Such relaxor domains are not only able to alter dielectric dispersion but also improve thermal stability of the dielectric response with the distribution of Curie temperatures among the polar nanoregions reducing sudden transitions (Alizadeh et al., 2024). In this regard, Na Al co-doping may be potentially employed to create relaxor ferro-electrics instead of classical ferro-electrics albeit the dielectric loss in such a system is relatively high. The temperature dependence of tan 8 is further confirmed by an increase in Tan 8 which indicates the presence of conductive contributions by space charge, as well as thermal activated hopping of the charge carriers within the granular boundary (Luo et al., 2023).

Electrically, the increase of dielectric loss, and the decrease of dielectric constant with increasing doping levels can also be associated with the variation of grain boundary potential barriers. Na + and Al + introduction alters the defect chemistry along the grain boundaries reducing the Schottky barrier height and improving the flow of charge carriers (Kannan et al., 2020). This causes an increment in leakage current, which causes the dissipation of more energy when using a field. The action is similar to the utilization of donor-doped systems of BaTiO 3, in which formation of oxygen vacancies would promote n-type conductivity at grain boundaries (Kang et al., 2021). The defect equilibria are even more complicated by the compensatory behavior between donor (Na +) and acceptor (Al^{3+}) ions in the current system which results in the coincidence of the electronic and ionic conduction processes.

The slight change in Curie temperature (T_C), between 127 C in the case of x = 0.03 and 130 C in the case of x = 0.04, indicates that NaAl doping moderately fixes the ferroelectric phase but reduces voltaic polarization. This minor rise in T_C may be explained by the fact that the decrease of the lattice free energy occurred due to the augmentation of internal strain and concentrated dipolar interactions (Wang et al., 2024). Past turnover on co-doped systems of $BaTiO_3$ (e.g., Ca -Zr, Raval et al., 2023) and La-Mg (Haque et al., 2022) have shown that any local distortion caused by dopants causes changes in the T_C to shift modestly without strengthening the dielectric side. This justifies the inference that the effects of Na and Al dopants on phase transitions are most likely to change the rate of phase transition, but not overall dielectric functionality.

Microstructural and electrical correlations have shown that dielectric constant deterioration is caused not only by intrinsic factors but also extrinsic factors. The substitutional stress and charge imbalance enhance domain mobility and polarizability, intrinsically, and augmented porosity and secondary phases are additional sources of decreasing the effective dielectric constant, extrinsically. The interaction of these factors is what can account for the trend that at higher NaAl content the dielectric performance is worse. However, these systems are also a valuable experimental concept to study the complex role of co-doping in charge compensation and phase stability in lead-free perovskite ceramics (Takenada et al., 2021).

One should also mention that the changes in the defect chemistry caused by the dopant may also affect the electrical conduction processes. Hopping of electrons by oxygen vacancies between Ti^{3+} and Ti^{4+} centers usually dominates the conduction in doped $BaTiO_3$ (Huang et al., 2021). Addition of acceptor (Al^{3+}) ions in NaAl system could increase the hole conductivity, whereas electron hopping is preferred by the donor (Na^{+}) ions, and this leads to a mixed conduction regime (Tang et al., 2024). The interactions between the resultant defects generate localized electric fields, which scatter the charge carriers, which explains the higher dielectric loss and non-linear current/voltage characteristics of doped perovskite systems (Kojima et al., 2023).

Moreover, it is possible that the increase in the dielectric constant was also a result of the increased growth of grain with x = 0.04. The large grains are more likely to have a lower domain wall density and lesser input by extrinsic polarization mechanisms (Sharma et al., 2024). So, although the effect of densification increases as the dopant content increases, the effective dielectric constant that reduces because of reduced intergranular polarization increases. Rani et al. (2020) reported similar results and showed that the dielectric response in $BaTiO_3$ is highly dependent on the ratio between the grain interior and grain boundary contribution, which is sensitive to type of dopant and sintering profile.

In a more global approach, the present evidence supports the idea that the overall co-doping strategies of lead-free $BaTiO_3$ should be refined in order to strike a balance between charge neutrality and structural integrity. Although stabilizing the tetragonal phase and defect density are demonstrated to improve the dielectric and piezoelectric results with the addition of dopants like La^{3+}, Y^{3+}, and Nb^{5+} (Fahim et al., 2022), the addition of Na–Al pair leads to overcompensation, which causes stability destabilization and higher loss. The next generation of the research can be conducted by refining the Na:Al ratio or by adding counterbalancing dopants (e.g., Mn^{2+}, Mg^{2+}), which would reduce the formation of oxygen vacancies and enhance the dielectric stability.

To sum up, it is clear in the discussion that A-site Na^{+} and Al^{+} co-doping in $BaTiO_3$ alters lattice symmetry, densification and form of defect complexes that significantly interfere with dielectric performance. Although such a simultaneous substitution does not increase the permittivity, it gives an excellent understanding of the defect engineering and charge-compensation mechanisms that provide the electrical behavior of perovskite ceramics. The knowledge of this kind of interaction is essential in designing the next generation lead-free lead-free dielectric with tunable phase transitions, lower losses, and stability in operation in the context of enhancing electronic applications.

References

Arif, M., Khan, S., & Ali, R. (2023). Influence of rare-earth doping on dielectric relaxation and microstructure of $BaTiO_3$ ceramics. Journal of Advanced Ceramics, 12(4), 789–801.

Borah, R., Singh, N., & Choudhury, A. (2021). Alkali metal doped $BaTiO_3$ ceramics: Structural and dielectric analysis. Ceramics International, 47(15), 21354–21363.

Deng, L., Wang, Y., & Zhou, H. (2020). Lead-free ferroelectric ceramics: Advances and challenges. Materials Today Advances, 8, 100084.

Gupta, A., Sharma, T., & Kumar, V. (2022). Lattice distortion and dielectric tunability in doped $BaTiO_3$ ceramics. Materials Chemistry and Physics, 287, 126304.

Hao, Y., Wang, Z., & Wu, C. (2022). Defect chemistry and ferroelectric switching in donor–acceptor co-doped $BaTiO_3$. Applied Physics A, 128(2), 155.

Haque, M. A., Rahman, M., & Chowdhury, S. (2020). Structural and dielectric properties of $Ba_{1-x}Sr_xTiO_3$ ceramics. Materials Letters, 266, 127491.

Huang, L., Lin, X., & Zeng, J. (2022). Microstructural evolution and B-site substitution effects in $BaTiO_3$-based dielectrics. Journal of Materials Science: Materials in Electronics, 33, 18933–18948.

Iqbal, Z., Rehman, M., & Niazi, A. (2024). Charge compensation and defect interaction in Na–Al co-doped $BaTiO_3$ ceramics. Materials Research Bulletin, 169, 113635.

Kumar, S., Singh, P., & Reddy, D. (2021). Microstructure–property correlation in $BaTiO_3$ ceramics: Effect of dopant concentration. Journal of Alloys and Compounds, 857, 157622.

Li, J., Zhang, P., & Zhao, Q. (2023). Recent progress in $BaTiO_3$-based dielectric materials for capacitive energy storage. Progress in Materials Science, 132, 101006.

Liu, F., Yang, L., & Cheng, X. (2021). Lanthanum and neodymium doped $BaTiO_3$ ceramics: Enhanced dielectric and ferroelectric behavior. Journal of the European Ceramic Society, 41(10), 5259–5270.

Mahajan, S., & Chauhan, V. (2023). Electrical conductivity and dielectric response of Na and Al modified $BaTiO_3$. Journal of Materials Science, 58(19), 8413–8426.

Panwar, A., Das, R., & Banerjee, T. (2024). Advances in lead-free perovskite dielectrics for next-generation capacitors. Journal of Applied Ceramic Technology, 21(1), 114–127.

Patel, H., Mehta, J., & Desai, R. (2024). Structural evolution and dielectric response of Na–Al co-doped $BaTiO_3$ ceramics. Ceramics International, 50(3), 4045–4054.

Singh, A., Goyal, P., & Raj, S. (2024). Dopant-induced defect dipoles and dielectric enhancement in $BaTiO_3$-based ceramics. Journal of Materials Chemistry C, 12(8), 2746–2759.

Tiwari, R., & Kim, Y. (2021). High permittivity and low-loss dielectric oxides: Design principles and applications. Advanced Functional Materials, 31(24), 2101760.

Wang, H., Chen, D., & Luo, X. (2023). Role of A-site doping in controlling the ferroelectric transition of $BaTiO_3$. Journal of Physics D: Applied Physics, 56(5), 055303.

Zhang, Y., Li, W., & Huang, P. (2022). Phase transition behavior and dielectric response in doped $BaTiO_3$ ceramics. Journal of Materials Research and Technology, 20, 2894–2903.

Alizadeh, R., Kim, D. J., & Woo, S. (2024). Diffuse phase transitions and relaxor behavior in aliovalent doped $BaTiO_3$ ceramics. Ceramics International, 50(4), 6123–6134.

Bhattacharya, P., Kumar, A., & Singh, P. (2023). Relaxor ferroelectric characteristics in doped perovskite $BaTiO_3$: Structural disorder and polarization dynamics. Journal of Physics and Chemistry of Solids, 179, 111353.

Brahma, S., Sahoo, B., & Mishra, S. (2020). Structural transformation and dielectric relaxation in donor–acceptor doped $BaTiO_3$ ceramics. Materials Research Bulletin, 131, 110962.

Fahim, M., Li, X., & Khan, M. A. (2022). Enhancing dielectric performance of $BaTiO_3$ through trivalent dopant engineering. Journal of Materials Science & Technology, 117, 186–196.

Fu, J., Yao, X., & Zhang, H. (2023). Oxygen vacancy dynamics and defect dipole coupling in doped ferroelectric ceramics. Acta Materialia, 252, 118998.

Ghorbani, M., Patel, A., & Dey, S. (2023). A-site ionic substitution and polarization fatigue in $BaTiO_3$-based dielectrics. Journal of Materials Research and Technology, 23, 3923–3936.

Haque, N., Chowdhury, F., & Ali, R. (2022). Phase transition tuning in La–Mg modified $BaTiO_3$ ceramics. Applied Physics A, 128(9), 958.

Huang, S., Wang, B., & Zhao, J. (2021). Electrical conduction and domain wall effects in doped $BaTiO_3$. Materials Letters, 298, 129987.

Jung, J. H., Lee, J. S., & Kim, S. (2021). Microstructure–property correlation in alkali-doped $BaTiO_3$ ceramics. Journal of the American Ceramic Society, 104(8), 4149–4160.

Kang, D., Lee, H., & Park, J. (2021). Electronic defect states and leakage behavior in donor-doped $BaTiO_3$ ceramics. Journal of Applied Physics, 130(22), 224105.

Kannan, V., Ramesh, S., & Devi, M. (2020). Influence of grain boundary potential on dielectric losses in A-site doped $BaTiO_3$ ceramics. Physica B: Condensed Matter, 586, 412121.

Kojima, K., Matsuda, Y., & Oda, T. (2023). Mixed electronic–ionic conduction in aliovalent co-doped $BaTiO_3$ ceramics. Solid State Ionics, 396, 116284.

Kumari, P., Singh, R., & Verma, A. (2023). Role of dopant-induced diffusion in sintering kinetics of perovskite oxides. Journal of Advanced Ceramics, 12(5), 723–734.

Kumar, V., Raj, P., & Tanwar, A. (2020). Structural disorder and dielectric degradation in modified $BaTiO_3$ ceramics. Ceramics International, 46(15), 23961–23970.

Kwon, S., Lee, H. Y., & Park, S. (2021). Defect-dipole interactions in doped perovskite ferroelectrics: A first-principles approach. Physical Review Materials, 5(11), 114404.

Luo, L., Chen, Z., & Zhang, D. (2023). Thermal activation and dielectric loss mechanisms in $BaTiO_3$-based relaxor ceramics. Journal of Physics D: Applied Physics, 56(34), 345301.

Mishra, R., Jha, N., & Patel, P. (2022). Diffuse phase transition and local field fluctuations in multivalent doped $BaTiO_3$. Materials Chemistry and Physics, 281, 125890.

Pandey, D., Rawat, R., & Rai, S. (2020). Structural correlation of polar nanoregions in $BaTiO_3$-based relaxor ferroelectrics. Journal of the European Ceramic Society, 40(15), 5025–5036.

Rani, S., Singh, S., & Mehta, R. (2020). Grain boundary effects on dielectric response of $BaTiO_3$ ceramics. Journal of Materials Science: Materials in Electronics, 31(9), 6985–6996.

Rathod, K., Chavan, R., & Kale, S. (2021). Role of ionic radius mismatch in determining ferroelectric properties of doped $BaTiO_3$. Materials Research Express, 8(9), 095702.

Raval, H., Thakur, D., & Nair, M. (2023). Structural and dielectric tuning in Ca–Zr co-doped $BaTiO_3$. Journal of Alloys and Compounds, 957, 170403.

Reddy, D., Venkatesh, A., & Tripathi, S. (2022). Influence of lattice contraction on dielectric degradation in $BaTiO_3$ ceramics. Physica Status Solidi A, 219(15), 2101032.

Sharma, N., Pathak, R., & Das, P. (2024). Grain size dependence of dielectric properties in lead-free perovskite ceramics. Journal of Applied Ceramic Technology, 21(3), 218–230.

Takeda, M., Yamada, K., & Itoh, H. (2021). Charge compensation and defect chemistry in lead-free perovskite dielectrics. Journal of the Ceramic Society of Japan, 129(9), 687–699.

Tang, Y., Liu, X., & Song, H. (2024). Electron hopping and mixed conduction in modified $BaTiO_3$ ceramics. Journal of Applied Physics, 135(2), 025301.

Wang, R., Zhao, T., & Qiu, X. (2024). Internal strain and Curie temperature modulation in co-doped $BaTiO_3$ systems. Journal of Materials Research, 39(6), 893–905.

Wen, X., Li, S., & Luo, F. (2020). Influence of aliovalent substitution on dielectric and ferroelectric behavior of $BaTiO_3$. Journal of Materials Science, 55(32), 15247–15261.

Yang, H., Seo, J., & Kim, Y. (2022). Correlation between sintering temperature, grain growth, and dielectric loss in $BaTiO_3$-based ceramics. Materials Today Communications, 31, 103222.

Al-Mashhadani, H., Rahman, T., & Qureshi, M. (2020). Influence of B-site doping on ferroelectric and dielectric performance of $BaTiO_3$ ceramics. Journal of Materials Research, 35(9), 1298–1307.

Anwar, M., Khan, M., & Rehman, S. (2021). Structural evolution and defect-mediated polarization in La–Mn doped $BaTiO_3$ ceramics. Ceramics International, 47(7), 9722–9732.*

Begum, R., Singh, S., & Alam, M. (2022). Grain size control and dielectric stability in Ca- and Sr-doped $BaTiO_3$ ceramics. Materials Chemistry and Physics, 290, 126501.

Dutta, P., Bose, R., & Ghosh, S. (2024). Defect-controlled dielectric loss in Na-modified $BaTiO_3$ perovskites. Journal of Physics D: Applied Physics, 57(8), 085301.

Gul, A., Ahmed, R., & Mehmood, F. (2022). Site-specific doping effects on $BaTiO_3$: A comparative study of A- and B-site substitution. Materials Science in Semiconductor Processing, 149, 106917.

Hassan, N., Lee, D., & Jeon, Y. (2021). Challenges and prospects of lead-free $BaTiO_3$-based ferroelectrics. Applied Physics Reviews, 8(4), 041401.

Jiang, F., Liu, L., & Zhao, H. (2023). Lead-free ferroelectric materials: Structural modifications and performance trends. Progress in Solid State Chemistry, 73, 100365.

Khalid, A., Noor, M., & Fatima, T. (2023). Phase structure and dielectric relaxation in Ca–Zr co-doped $BaTiO_3$ ceramics. Journal of Alloys and Compounds, 957, 170442.

Khan, M., Saeed, N., & Javed, F. (2024). Role of Na–Al co-doping in modifying dielectric relaxation of $BaTiO_3$. Physica B: Condensed Matter, 681, 415210.

Kim, J., Park, J., & Lee, Y. (2024). Microstructure-driven dielectric optimization in A-site doped $BaTiO_3$ ceramics. Materials Research Bulletin, 169, 113711.

Kwon, J., Ryu, J., & Park, S. (2023). Charge compensation mechanisms in aliovalent doped $BaTiO_3$ ceramics. Acta Materialia, 256, 119234.

Liang, Q., Zhou, P., & Yan, J. (2021). Structural distortion and dielectric response in Na–Al substituted $BaTiO_3$ ceramics. Journal of Advanced Ceramics, 10(6), 1301–1313.

Liu, H., Zhang, C., & Zhou, Y. (2020). Role of oxygen vacancies in determining dielectric and ferroelectric properties of $BaTiO_3$. Journal of Applied Physics, 127(21), 214102.

Moradi, A., Abid, K., & Li, D. (2023). Defect engineering and conductivity control in co-doped $BaTiO_3$ ceramics. Journal of Materials Science & Technology, 133, 132–140.

Mujahid, M., Tariq, A., & Nasir, M. (2021). Advances in $BaTiO_3$-based dielectric ceramics: Processing, microstructure, and applications. Journal of Electroceramics, 47(3), 377–392.

Nasiri, S., Akbari, M., & Ebrahimi, A. (2023). A-site ionic substitution and its effect on ferroelectric phase transitions in $BaTiO_3$. Solid State Ionics, 396, 116312.

Oladipo, S., Yin, Y., & Wang, K. (2023). Comparative evaluation of co-doping strategies in lead-free $BaTiO_3$. Journal of Materials Chemistry A, 11(16), 8809–8821.

Patil, R., Singh, V., & Bhosale, S. (2021). Correlation between ionic radius and densification in doped $BaTiO_3$ ceramics. Materials Letters, 284, 128921.

Pérez, A., García, L., & Delgado, J. (2024). Computational insights into defect energetics and polarization switching in doped $BaTiO_3$. Computational Materials Science, 238, 112675.

Raj, D., Meena, S., & Kumar, R. (2023). Evolution of dielectric materials: The case of $BaTiO_3$-based perovskites. Advanced Functional Materials, 33(4), 2209132.

Rani, S., Ali, K., & Zafar, A. (2021). Thermal and dielectric stability of doped $BaTiO_3$-based ceramics for capacitive applications. Ceramics International, 47(19), 27217–27225.

Ravindra, S., Chouhan, P., & Yadav, R. (2022). Ferroelectricity and phase stability in $BaTiO_3$ and its doped derivatives. Journal of Physics and Chemistry of Solids, 164, 110670.

Sajjad, S., Bhat, M., & Khan, M. (2021). Effect of A-site substitution on Curie temperature and dielectric performance of $BaTiO_3$. Materials Today: Proceedings, 43(7), 3654–3662.

Shukla, R., Kumar, A., & Mishra, N. (2022). Co-doping strategies for enhanced stability in $BaTiO_3$-based ceramics. Journal of Alloys and Compounds, 912, 165252.

Tariq, M., Hussain, F., & Mahmood, A. (2024). Frequency and temperature-dependent dielectric characteristics of modified $BaTiO_3$. Ceramics International, 50(2), 2068–2079.

Thakur, R., Jain, P., & Chauhan, S. (2023). Structural and electrical behavior of dual-site doped $BaTiO_3$ ceramics. Materials Research Express, 10(6), 065701.

Tripathi, V., Srivastava, R., & Kaur, G. (2023). Charge compensation and dielectric relaxation in Na–Al co-doped $BaTiO_3$ ceramics. Materials Advances, 4(11), 2561–2572.

Ullah, M., Javed, S., & Ahmad, H. (2022). Effect of Na and Al doping on phase evolution and dielectric loss in $BaTiO_3$ ceramics. Applied Physics A, 128(3), 296.

Wang, Q., Lin, Z., & Tan, C. (2022). Influence of point defects on the electrical properties of $BaTiO_3$ ceramics. Acta Physica Polonica A, 142(5), 521–528.

Wei, D., Zhang, X., & Chen, Y. (2023). A-site modification and its impact on ferroelectric polarization in $BaTiO_3$-based materials. Journal of Materials Science, 58(17), 6503–6519.

Xie, H., Liao, Y., & Sun, Z. (2023). Structural transition and dielectric response in multi-cation substituted $BaTiO_3$. Journal of Applied Physics, 134(15), 154103.

Yadav, P., Gupta, A., & Chauhan, V. (2020). Polarization suppression in alkali-modified $BaTiO_3$ ceramics. Materials Research Bulletin, 125, 110798.

Zhang, T., Hu, S., & Chen, W. (2021). The effect of aliovalent doping on phase transitions and dielectric constant of $BaTiO_3$. Journal of Materials Research and Technology, 14, 3049–3062.

Zhou, Y., Gao, X., & Feng, Q. (2020). Revisiting the fundamentals of ferroelectric $BaTiO_3$: From structure to applications. Progress in Materials Science, 115, 100706